Cell, Vol. 88, 845–854, March 21, 1997, Copyright ©1997 by Cell Press

RNA-Mediated RNA Degradation and Chalcone Synthase A Silencing in Petunia

M. Metzlaff, M. O'Dell,
P. D. Cluster,* and R. B. Flavell
John Innes Centre
Norwich Research Park
Colney, Norwich, NR4 7UH
United Kingdom

Summary

Transgenic Petunia plants with a *chsA* coding sequence under the control of a 35S promoter sometimes lose endogene and transgene chalcone synthase activity and purple flower pigment through posttranscriptional *chsA* RNA degradation. In these plants, shorter poly(A)$^+$ and poly(A)$^-$ *chsA* RNAs are found, and a 3′ end–specific RNA fragment from the endogene is more resistant to degradation. The termini of this RNA fragment are located in a region of complementarity between the *chsA* 3′ coding region and its 3′ untranslated region. Equivalent *chsA* RNA fragments remain in the white flower tissue of a nontransgenic Petunia variety. We present a model involving cycles of RNA–RNA pairing between complementary sequences followed by endonucleolytic RNA cleavages to describe how RNA degradation is likely to be promoted.

Introduction

The silencing of transgenes and of endogenous genes homologous to transgenes is a frequently observed phenomenon in plants (for an overview, see Meyer, 1995). The possible mechanisms of silencing may vary among the reported cases (Flavell, 1994; Matzke and Matzke, 1995). Sometimes they result in inhibition of transcription (Meyer and Heidmann, 1994); in other cases they act posttranscriptionally (De Carvalho Niebel et al., 1995; Depicker et al., 1996; Hamilton et al., 1996). The loss of chalcone synthase in Petunia hybrida flowers due to the introduction of *chalcone synthase A* (*chsA*) transgenes is apparently not associated with reduced transcription, as demonstrated by run-on transcription tests in isolated nuclei (Van Blokland et al., 1994). It therefore has been assumed to be due to posttranscriptional degradation of *chsA* RNA from both the endogene and the transgene *chsA* genes. This phenomenon has been called cosuppression (Napoli et al., 1990). Chalcone synthase is a key enzyme in anthocyanin biosynthesis, and the *chsA* genes are transcriptionally activated in the epidermal cells of flower petals (Martin, 1993). Loss of *chsA* RNA therefore leads to loss of anthocyanin pigment in petals, and white flower tissue is created instead of purple tissue.

A large number of transgenic Petunia plants with variant flower phenotypes have been described that contain transgenes consisting of Petunia *chsA* cDNA under the control of the cauliflower mosaic virus 35S promoter with two enhancer elements and the 3′ untranslated region (UTR) from the nopaline synthase gene of Agrobacterium tumefaciens (Napoli et al., 1990; Jorgensen, 1995; Jorgensen and Napoli, 1996; Jorgensen et al., 1996). Many of the transgenic plants have only white flowers, thus displaying complete phenotypic cosuppression. Others display cosuppression in floral sectors, and the white sectors are organized in specific patterns. Recently, Jorgensen et al. (1996) showed that the frequency and patterns of floral cosuppression in such Petunia plants are correlated with the number of transgenes and their arrangement in the genome. The patterns of cosuppression are inherited somatically and sometimes through meiosis. However, in other cases epigenetic changes occur in meristems and result in changes in the floral patterns of cosuppression (Jorgensen, 1995; Jorgensen and Napoli, 1996). Despite the extensive studies on the phenotypic expression of cosuppression and knowledge that the process apparently involves *chsA* RNA degradation (Van Blokland et al., 1994), little is understood about the precise changes in RNA levels in transformants displaying different extents of cosuppression and the mechanisms of specific RNA degradations.

In this report we describe changes in *chsA* RNA biology in leaves and flowers in Petunia plants that are induced as a consequence of introducing the *chsA* transgenes. From the amounts and structures of the *chsA* RNAs, we conclude that transgenic plants with purple or purple-white flowers can have elevated levels of endogene and transgene poly(A)$^+$ *chsA* RNAs, while plants with all-white flowers show substantial loss of endogene and transgene poly(A)$^+$ RNAs. Much of the *chsA* RNA is poly(A)$^-$, which we conclude is a product of a specific cleavage in the mRNA. A *chsA* endogene 3′ end–specific RNA fragment appears to be the last endogene RNA fragment to be degraded in tissue showing severe *chsA* cosuppression. An identical remaining *chsA* 3′ end fragment can be observed in the white flower tissue of plants, as it can in the nontransgenic Petunia variety Red Star, which carries purple-white patterned flowers (Mol et al., 1983); this observation indicates that the transgene RNA present in transgenic lines acts only as a trigger for the induction of an existing *chsA* RNA–specific, posttranscriptional control mechanism. We present a model based on RNA–RNA base pairing, when poly(A)$^-$ or aberrant RNAs are locally elevated, and involving specific endonucleolytic RNA cleavages to explain how *chsA* RNA degradation is likely to be promoted to cause phenotypic cosuppression.

Results

Amounts of *chsA* RNA Differ between Leaf and Flower Tissues and among Transformants with Different Floral Phenotypes

To determine the relative levels of *chsA* RNA in leaf and flower tissues of wild-type and selected transgenic

---

* Present address: Plant Breeding Laboratory, Faculty of Agriculture, Kyoto University, Kyoto 606–01, Japan.

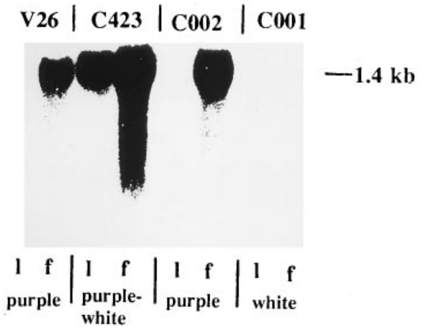

Figure 1. Northern RNA Analysis of Leaf and Flower Tissues of Wild-Type and Selected Transgenic Petunia Plants

Ten micrograms of total RNA was separated on a 1% agarose–20% formaldehyde gel, transferred onto a nylon filter, and hybridized with a ^{32}P-*chsA*-cDNA probe. The size of the *chsA* transcript and the flower phenotypes are indicated. l, leaves; f, flowers.

Petunia plants, we performed Northern RNA analyses (Figure 1) and RNA dot-blot analyses (data not shown). Both the Northern and the dot-blot analyses proved the high induction of *chsA* RNA levels in wild-type flowers relative to leaves (Figure 1, V26) and the strong reduction of *chsA* RNA in white flower tissue (Figure 1, C001). In this latter tissue only traces of *chsA* RNA could be detected by both analyses, whereas hybridization of the filter with ribosomal DNA proved that approximately equal amounts of total RNA were transferred onto the filter. The drastic reduction in the level of *chsA* RNA in white flower tissue shown in our Northern and dot-blot analyses is consistent with data published earlier for Petunia flower tissue with cosuppressed *chsA* genes (Napoli et al., 1990; Van der Krol et al., 1990; Van Blokland et al., 1994).

The total RNA analyses yielded two other findings. First, in purple flower tissue of the two transgenic lines C423 and C002, the level of *chsA* RNA was higher than in wild-type purple flower tissue. The observed elevation ranged between 20- to 40-fold, as estimated from a series of dot-blot analyses with dilutions of total RNA down to 0.015 μg. Second, the level of *chsA* RNA in leaf tissue of the unstable, purple-white flowering transgenic line C423 was much higher (>100-fold) than the expected very low levels in wild-type leaves and in leaves of stable purple (C002) or stable white (C001) flowering transgenic lines.

To investigate whether the presence of specific *chsA* RNA species in leaf and flower tissue correlates with specific phenotypes, we carried out endogene- and transgene-specific reverse transcriptase polymerase chain reaction (RT-PCR) analyses on total leaf and flower RNA preparations. By using specific oligonucleotides (normally 20-mers) as primers for cDNA synthesis and PCR amplifications, we differentiated between endogene and transgene *chsA* transcripts and between total *chsA* RNA and polyadenylated *chsA* RNA. The cDNA reactions were carried out on equal aliquots of RNA. This approach allowed quantitative comparisons to be made within and between genotypes. To aid the quantitative interpretation of PCR products, relatively few amplification cycles (normally 18) were carried out, followed by hybridization with a *chsA* cDNA probe. Where RT-PCR products could not be detected by hybridization, a high number of PCR amplification cycles (normally 35) was performed, followed by hybridization, to investigate whether very low levels of *chsA* RNAs were present.

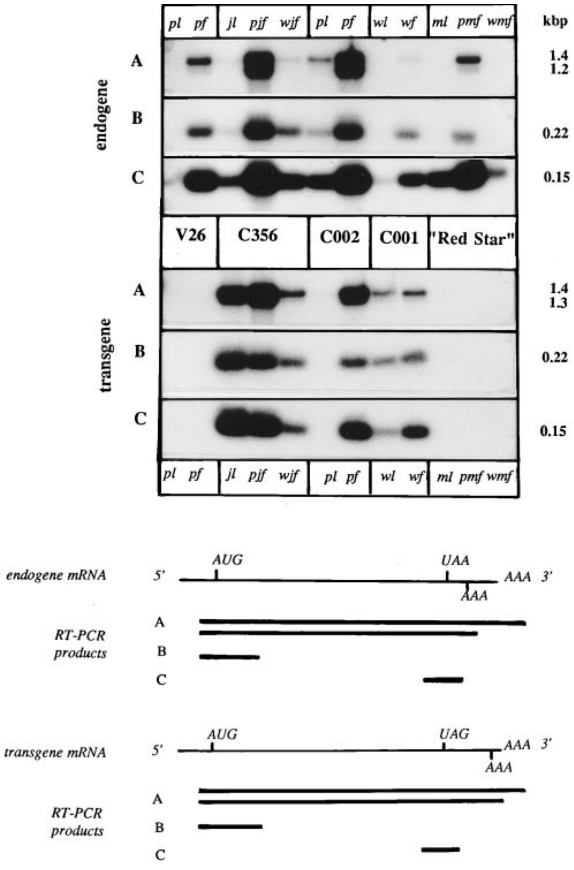

Figure 2. RT-PCR Performed on Total RNA Isolated from Leaf and Flower Tissues of Nontransgenic and Selected Transgenic Petunia Plants

Endogene and transgene *chsA* RNA–specific cDNAs were amplified by 18 cycles of PCR. The resulting PCR products were separated on either 1.5% (A) or 2.5% (B and C) agarose gels, transferred onto nylon membrane, and hybridized with a *chsA*-cDNA probe. The sizes of the RT-PCR products are indicated. V26 is the purple flowering wild-type line, Red Star a nontransgenic line with purple-white patterned flowers, C356 a transgenic line with purple-white patterned flowers, C002 a transgenic line with fully purple flowers, and C001 a transgenic line with all-white flowers. The type of tissue from which the total RNAs were isolated are labeled as follows: pl, leaf tissue of plants with fully purple flowers; pf, purple flower tissue; jl, leaf tissue of plants with purple-white patterned flowers; pjf or wjf, purple or white sectors, respectively, of purple-white patterned flowers; wl, leaf tissue of plants with fully white flowers; wf, white flower tissue; ml, leaf tissue of nontransgenic plants with purple-white patterned flowers; pmf or wmf, purple or white sectors, respectively, of nontransgenic purple-white flowers.

Figure 2 summarizes RT-PCR data for plants selected as representatives of three phenotypic groups: plants with stable phenotypes of all-purple flowers (C002, which is an epigenetic variant of C001; Napoli et al., 1990); plants with all-white flowers (C001); and plants with purple-white patterned flowers (C356). We compared the RT-PCR patterns for the transgenic lines with RT-PCR patterns obtained for total RNA isolated from leaf and flower tissue of wild-type V26 plants and from flowers similar to those of the Petunia variety Red Star. We decided to include this variety in our analyses because its flowers display purple and white sectors like those of the unstable purple-white flowering transgenic lines. To assay poly(A)$^+$ RNA we performed 3′ rapid amplification of cDNA ends (RACE) amplifications (Figure 2A; Frohman et al., 1988) using an oligo(dT)-adaptor primer. To display full-length *chsA* poly(A)$^+$ RNA and to differentiate between endogene and transgene poly(A)$^+$ cDNA, the adaptor oligonucleotide was used in combination with the 5′ UTR–specific oligonucleotides G995 and G996, respectively, for the 18 PCR cycles. A single RT-PCR product of 1.4 kb was expected for full-length poly(A)$^+$ RNAs, from both the endogene and the transgene. To detect any nonpolyadenylated *chsA* RNA in addition to poly(A)$^+$ RNA displayed by 3′ RACE, we primed other cDNA syntheses using identical RNA preparations with 5′ end– and 3′ end–specific oligonucleotides (Figures 2B and 2C, respectively). For the 5′ end–specific cDNA syntheses we used the oligonucleotide G2350, which is complementary to nucleotides 1360 to 1381 within the *chsA* coding region (numbering according to sequence file X14591 of the EMBL/GenBank/DDBJ databases). To distinguish between endogene and transgene 5′ ends, we amplified aliquots of the resulting cDNAs using the oligonucleotide G2350 in combination with the same oligonucleotides G995 or G996 that we used for the full-length poly(A)$^+$ RNA RT-PCR amplifications. The expected size of the resulting RT-PCR products was 220 bp in both cases. The 3′ end–specific cDNA syntheses were primed either with oligonucleotide G1607, which is complementary to the first 20 nucleotides of the endogene 3′ UTR, or G1607T, which is complementary to the first 20 nucleotides of the transgene 3′ UTR. Both 3′ end–specific cDNAs were PCR amplified with either G1607 or G1607T in combination with oligonucleotide G3280, which is specific for positions 3611–3634 within the *chsA* coding region. The expected size for both RT-PCR products was 150 bp.

Our analyses showed that *chsA* poly(A)$^+$ RNA can be displayed by RT-PCR at high levels in all types of purple flower tissue (Figure 2, pf, pjf, and pmf). In the case of wild-type and Red Star flower tissue, only endogene-specific RT-PCR products were obtained, whereas both types of *chsA* poly(A)$^+$ RNA RT-PCR products, endogene and transgene, were present in transgenic purple flower tissue. However, in the flower tissues of these transgenic genotypes the level of endogene *chsA* poly(A)$^+$ RNA was clearly elevated in comparison to levels found in wild-type and Red Star–type flower tissue. Thus, here the coexpression of both types of *chsA* genes appears to deregulate the control of endogene *chsA* poly(A)$^+$ RNA levels. Furthermore, when the level of *chsA* poly(A)$^+$ RNA is elevated, shorter poly(A)$^+$ RNA RT-PCR products with sizes of 1.2 kb for the endogene RNA and 1.3 kb for the transgene RNA become abundant. The shorter endogene poly(A)$^+$ RNA product can be observed as a minor component in RT-PCR analyses performed with RNA from wild-type and Red Star–type flower tissue. We assume therefore that the 1.2 kb RT-PCR product reflects an enhanced *chsA* RNA-specific modification occurring as a consequence of *chsA* RNA accumulation. For white flower tissue of the transgenic lines (Figure 2, wjf, wf, and wmf) almost no endogene and only low levels of transgene *chsA* poly(A)$^+$ RNA RT-PCR products were found. This result reflects the strong reduction of *chsA* poly(A)$^+$ RNA in all-white flower tissue and is consistent with the loss of pigmentation in this tissue.

Our RT-PCR analyses also proved that the level of endogene *chsA* poly(A)$^+$ RNA in leaves is very low. However, in plants of the stable purple flowering transgenic line C002, the level of endogene *chsA* poly(A)$^+$ RNA was clearly elevated in leaves but no transgene *chsA* poly(A)$^+$ RNA could be detected. In contrast, in leaf tissues of the unstable purple-white flowering line C356 and the stable white flowering line C001, relatively high amounts of transgene *chsA* poly(A)$^+$ RNA product could be displayed by RT-PCR. The amounts were especially high in plants of the unstable purple-white flowering line. From this we conclude that transgene *chsA* poly(A)$^+$ RNA is the main component of the high levels of *chsA* RNA in leaf tissue of unstable purple-white flowering plants observed earlier in our Northern analyses (Figure 1). The leaves of all of the white flowering transformants that we assayed had low levels of transgene RNA. This supports the conclusion that loss of *chsA* RNA also occurs in the stems and leaves of plants that display cosuppression of *chsA* in flowers. The state of cosuppression in flowers is therefore likely to be determined by the properties of somatic cells long before flower formation.

Most of the Surviving *chsA* Transcripts in Flower Tissue Showing Severe Cosuppression Are Not Polyadenylated, and a Portion of the 3′ End of the Endogene *chsA* RNA Survives Degradation Preferentially

The data we obtained for the 5′ and 3′ end–specific RT-PCR analyses of the endogene and transgene *chsA* total RNA confirmed in general our observations of elevated or reduced levels of *chsA* poly(A)$^+$ RNAs in defined leaf and flower tissues of transgenic plants, but they also revealed other features. In white flower segments of C356, the ratio of poly(A)$^+$ 1.4 kb endogene RNA fragments to the 0.22 kb 5′ end fragments and 0.15 kb 3′ end fragments was low, relative to that in C356 purple flowers. This indicates that most of the *chsA* endogene RNA fragments are poly(A)$^-$, and the 1.4 kb fragments appear to be more sensitive to the degradation processes than other shorter *chsA* RNA fragments.

The white flower tissue of C001 also had reduced levels of the 1.4 kb poly(A)$^+$ RNA relative to C002, and here the 0.22 kb 5′ fragments were also relatively reduced. In the white flower tissue of Red Star, only 3′ end fragments could be detected. There was variation in the extent of total *chsA* RNA reduction, endogene and transgene, and varying residual levels of full-length, 5′, and 3′ fragments, but 3′ fragments always seemed to be the last to disappear from the complement of RNAs. This situation also was observed in leaf tissue of Red Star (Figures 2A–2C). Here the levels of the 3′ end fragments were much higher than in V26.

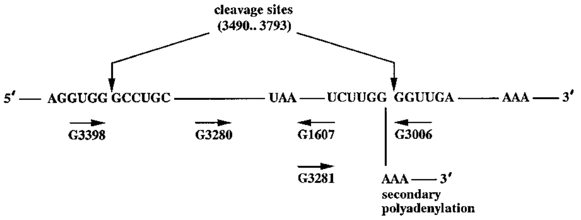

Figure 3. Sequence of Specific RNA Termini Located at the Endogene *chsA* 3′ End

The sequences surrounding identified termini at the endogene *chsA* 3′ end are shown. The numbers of the first 5′ nucleotide (3490) and the last 3′ nucleotide (3793) of the RNA fragment that are more resistant to degradation in vivo are given according to the numbering in sequence file X14591 of the EMBL/GenBank/DDBJ databases. The stop codon UAA and the secondary poly(A) site are indicated, as are the numbers and location of oligonucleotides used in 3′ end–specific RT-PCR amplifications.

The Endogene *chsA* RNA 3′ End Fragments That Resist Degradation Carry Specific 5′ and 3′ Termini Located in a Region of RNA–RNA Complementarity

The discovery that most *chsA* endogene RNA fragments in white flower tissue (and leaves) are not full-length poly(A)$^+$ and that 3′ end fragments appear to survive more than 5′ end fragments suggested, first, that there may be specific cleavage sites within the *chsA* endogene RNA, and second, that the 3′ end fragments may adopt a structure that is more resistant to RNases. We therefore identified the 3′ and 5′ ends of the 3′ fragments that are most resistant to RNases in white flower tissue. To do this we performed linear PCR reactions toward the *chsA* RNA 3′ end and primer extension reactions toward the 5′ end from known positions and assayed the sizes of the predominant products on gels. As template for the linear PCR amplifications we used poly(A)$^+$ cDNA and labeled primer G3281, which is specific for the first 20 nucleotides of the endogene *chsA* 3′ UTR (Figure 3). In the primer extension reactions performed on total RNA we used oligonucleotide G1607, which is complementary to the first 20 nucleotides of the endogene *chsA* 3′ UTR. The positions of the location of the 5′ and 3′ termini derived from the sizes of major bands of primer extension and linear PCR reactions in white flower tissue are indicated in Figure 3. To verify precisely the terminal bases, the regions surrounding the termination PCR products were sequenced, and the products of the sequencing reactions and primer extensions and PCR reactions were compared on a phosphonoacetic acid (PAA) sequencing gel. The terminal sequences obtained ("cleavage sites" in Figure 3) have been compared with other published RNA truncations points and endonucleolytic cleavage sites. Consistent with the other sequences the last nucleotide is G and the termini are within AU-rich regions (Table 1). The identified termini imply that the remaining *chsA* fragments are 304 bases long. The 3′ termination of the 304-base *chsA* RNA fragment deduced from sequencing and of the shorter (1.2 kb) *chsA* poly(A)$^+$ RNA observed earlier in our 3′ RACE experiments (Figure 2A) are identical (data not shown). From this we conclude that identical site-specific endonucleolytic cleavages occur in the formation of both classes of RNA.

To verify that most *chsA* endogene RNA is poly(A)$^-$ due to cleavage at the specific 3′ cleavage site and that some of the RNA molecules are also cleaved at the 5′ site to leave 304-base RNAs, a further series of experiments was conducted on RNA preparations from different tissues from various genotypes. Those from Red Star are shown in Figure 4. Using total RNA isolated from leaf, purple flower, and white flower tissue of Red Star, we primed the three cDNA syntheses with oligonucleotide G3006, which is complementary to the first 20 nucleotides downstream of the defined 3′ UTR cleavage site (Figure 3). In subsequent PCR amplifications of aliquots of the cDNAs this oligonucleotide was combined either with oligonucleotide G3398, which is specific for the first 20 nucleotides upstream of the observed 5′ termination at the *chsA* 3′ end (Figure 4A), or with oligonucleotide G3280, which is located inside the remaining *chsA* RNA 3′ fragment (Figure 4C). In both cases a major RT-PCR product was obtained only for the purple flower tissue RNA and not for the leaf tissue or white flower tissue RNAs. In Figure 4, lanes B and D, the cDNA synthesis was primed with oligonucleotide G1607, which is complementary to the first 20 nucleotides of the endogene *chsA* 3′ UTR and is located inside the remaining *chsA* RNA 3′ fragment. For PCR amplifications this oligonucleotide was again combined with G3398 located outside or G3280 located inside the remaining RNA fragment. The quantity of PCR products was higher for the purple flower RNA than for the leaf or white flower RNAs, reflecting the higher levels of *chsA* RNA in flowers. The amount of PCR products obtained using a primer downstream of the 3′ cleavage site (Figures 4A and 4C) were much lower than those obtained using primers upstream of the 3′ cleavage site. This finding confirms that a high proportion of all *chsA* endogene RNAs, in all tissues, terminate at this site and are poly(A)$^-$. The ratios of fragments amplified with the 5′ primer outside versus inside the 5′ cleavage site (Figures 4B and 4D), as judged by hybridization ratios in the autoradiograph, were similar in the leaf and purple flower tissue, indicating that many but not necessarily all of the RNAs do not have 5′ ends at the 5′ cleavage site. The equivalent ratio of amplified fragments (Figures 4B and 4D) from white flower tissue is, however, much lower than for leaf or purple flower tissue. In equivalent experiments using RNAs from some other white flower genotypes (data not shown), considerably lower ratios were seen. We therefore conclude from screening many genotypes that under conditions of severe cosuppression—that is, when most of the *chsA* endogene RNA is degraded—a high proportion of the remaining *chsA* endogene RNA consists of 304- base 3′ end fragments.

We investigated the secondary structure of the 3′ end of the *chsA* RNA by computer-based folding analyses in the program FOLDRNA (Zuker and Stiegler, 1981). It showed extensive secondary structures (Figure 5). We noted that in all of the putative secondary structures generated, the termini of the 304-base *chsA* RNA fragment are located within a 43-base paired segment showing 80% complementarity between a *chsA* 3′ coding region segment and the *chsA* 3′ UTR (Figure 5). Both fragment termini are also located close to bases of intrastrand loops.

Table 1. Truncation Points in the 3′ Region of *chsA* RNA (A) in Comparison with Two Published Cases of mRNA Truncations (B)

A	Endogene *chsA* 3′ UTR	5′-UUGUUUCUUGG↓GGUUG-3′
	chsA 3′ coding region	5′-UUGCUCAUCCAGG↓UGGGCCU-3′
	Transgene *chsA* 3′ *nos* UTR	5′-UGAUUAUCAUA↓UAAUUU-3′
B	Truncation points in the open reading frame of the tobacco etch virus coat protein RNA (Goodwin et al., 1996)	5′-GAAACCAAUGG↓UUGA-3′ 5′-GGUCUACAGAG↓AAACA-3′
	Endonucleolytic cleavage site in the 3′ UTR of human transferrin receptor mRNA (Binder et al., 1994)	5′-AUAAAG↓AACAAGGUGUUU-3′

The Complementarity between a Segment at the 3′ End of the *chsA* Coding Region and the *chsA* 3′ UTR Allows In Vitro Formation of RNA Duplexes That Are Not Degraded by a Double-Stranded RNA–Specific Endonuclease

From sequencing data of the 5′ and 3′ termination points at the *chsA* 3′ end and the putative structural features surrounding these terminations we postulated that double-stranded RNA (dsRNA)–specific endonucleases may be involved in the formation of the 304-base RNA fragment by *chsA* RNA-specific degradation processes. To test this hypothesis, we carried out the in vitro experiment documented in Figure 6. Both complementary regions of the *chsA* endogene 3′ end, the segment of complementarity within the 3′ coding region (positions 3467– 3532 in sequence file X14591 of the EMBL/GenBank/DDBJ databases), and the complete 3′ UTR (positions 3743–3970), were separately integrated into the in vitro transcription vector pSPT18 (Boehringer Mannheim), from which the recombinant plasmids pCC9 and pET5 resulted. The inserts were transcribed in vitro by using either T7 or SP6 RNA polymerase. In Figure 6, lanes A and B, the ^{32}P-labeled sense transcripts of the *chsA* 3′ UTR were annealed in vitro with a 10-fold excess of unlabeled 3′ UTR antisense transcripts. An aliquot of this annealing reaction was incubated with RNase III at 30°C for 20 min (Figure 6B). RNase III is a dsRNA-specific E. coli enzyme (Li et al., 1993) and was a gift from Dr. A. Nicholson (Wayne State University). In Figure 6, lanes C and D, the ^{32}P-labeled sense transcripts of the segment of complementarity at the *chsA* 3′ end of the coding region were annealed with a 10-fold excess of unlabeled sense transcripts of the *chsA* 3′ UTR. An aliquot of this annealing reaction was also incubated with RNase III. All four reactions were separated on a 5% nondenaturing PAA gel and exposed to X-ray film. In both annealing reactions without subsequent RNase III incubation (Figure 6, lanes A and C), bands with lower mobility than the ^{32}P-labeled in vitro transcripts could be observed. From this we conclude that in both reactions complex RNA structures have formed. The smear of radioactive products observed is presumably due to the diversity of complex dsRNA structures. Aliquots of both annealing reactions were incubated with RNase III. All of the complex RNA structures were degraded in the case of the self-annealed 3′ UTR transcripts (Figure 6, lane B), but where the *chsA* coding and 3′ UTR transcripts were mixed, the smear of products disappeared but a product remained with higher mobility than the major products present before RNase III treatment (Figure 6, lane D). We therefore conclude that the complementary coding and 3′ UTR RNA sequences can interact to form a structure that may have a cleavage site for RNase III but most of which is resistant to RNaseIII. The structure is therefore different from that formed when completely complementary RNA sequences are reannealed.

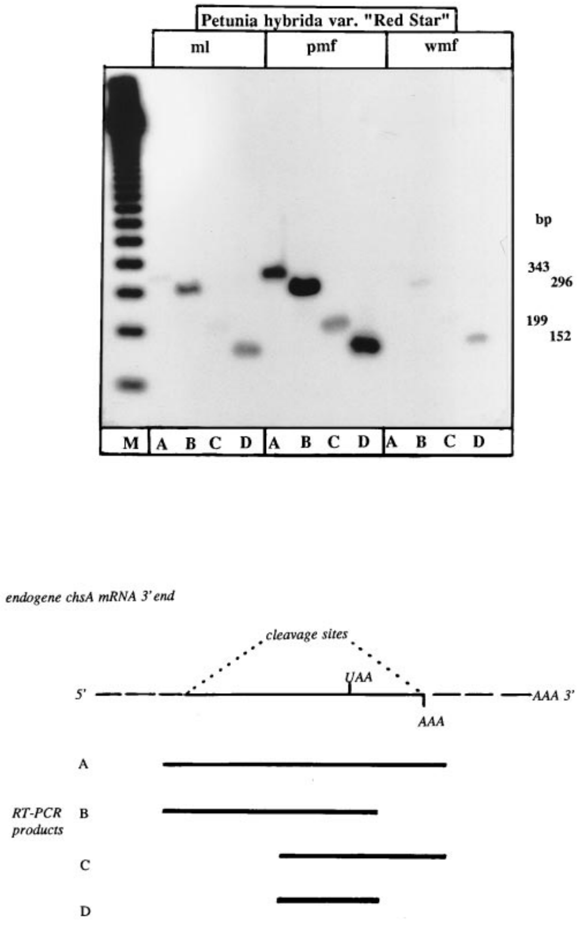

Figure 4. RT-PCR Patterns Obtained for the Endogene *chsA* 3′ End

RT-PCR amplifications were carried out on total RNA isolated from leaf tissue (ml) and purple (pmf) or white (wmf) flower tissue of the nontransgenic Petunia line Red Star. The sizes of the resulting RT-PCR products are indicated. The following oligonucleotide combinations were used for the RT-PCR amplifications: A, G3006/G3398; B, G1607/G3398; C, G3006/G3280; and D, G1607/G3280. For the location of these oligonucleotides see also Figure 3. M, 100 bp marker.

Discussion

From our studies on three groups of transgenic plants—(1) those that produce only fully purple flowers and rarely

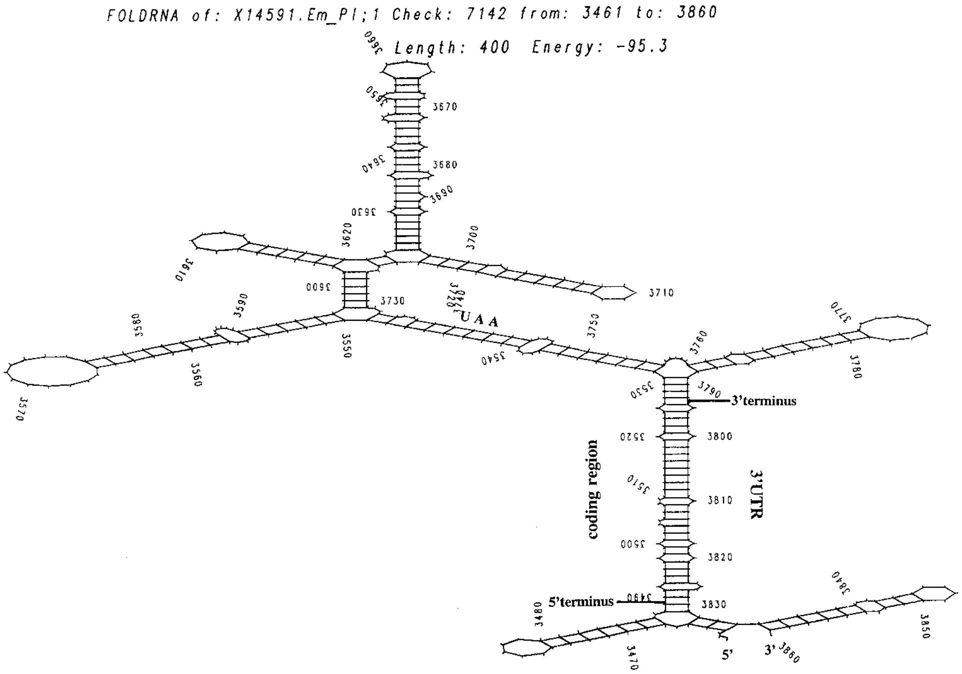

Figure 5. Computer-Based RNA Folding Analysis for the Endogene *chsA* 3′ End

The putative secondary structure of the last 400 nucleotides of the endogene *chsA* RNA 3′ end was obtained by using the program FOLDRNA (Zuker and Stiegler, 1981). The locations of the UAA stop codon and the 5′ and 3′ termini of the 304-base *chsA* RNA fragment that resists degradation are indicated.

show floral cosuppression, except sometimes in anthers; (2) those that are prone to cosuppression and regularly show characteristic white floral sectors and also produce somatic side shoots with fully white flowers; and (3) those that routinely produce all-white flowers and show full cosuppression—we can infer a series of steps that lead to cosuppression.

Transgenes Provoke a Range of Aberrations in Chalcone Synthase RNAs

When active transgenes do not promote floral cosuppression, as in group 1 plants, higher levels of poly(A)$^+$ endogene RNA accumulate in floral tissue and their own poly(A)$^+$ transcripts accumulate to high levels, too (Figure 2). The higher levels of endogene poly(A)$^+$ RNA imply that the transgenes either stimulate endogene transcription or reduce its degradation. Chalcone synthase RNA is known to be turned over relatively rapidly, and there is evidence that chalcone synthase levels are regulated in part posttranscriptionally (for a review see Martin, 1993). Thus, we favor the view that high concentrations of *chsA* RNA molecules can "titrate out" or inhibit some step in the *chsA* turnover process in flowers, thus reducing overall *chsA* RNA degradation rates. The high levels of endogene and transgene RNAs in these purple-flowered plants, which do not display cosuppression, suggest that high levels of *chsA* RNA alone are insufficient to promote cosuppression.

In the purple-white–flowered plants of group 2, which are prone to floral cosuppression, the *chsA* RNA levels can be typical of the group 1 stable purple types (Figure 2) or can have lower levels (unpublished data) that suggest that the RNA degradation system characteristic of cosuppression is already operating, during plant development, to some extent.

In group 3 plants, those showing full floral cosuppression, no or only low levels of full-length endogene and transgene *chsA* poly(A)$^+$ RNA survive. However, poly(A)$^-$ RNA fragments remain in white flower tissue, and when *chsA* RNA degradation is most extensive, 304-base sequences from the 3′ end of the RNA remain.

These results suggest that transformants suffer a continuum of aberrations, ranging from inhibition of *chsA* RNA degradation processes to extensive *chsA* degradation. The analyses of the *chsA* RNA surviving in the various transformants suggest that an early step in RNA degradation may be endonucleolytic cleavages at defined positions in the endogene and transgene 3′ UTRs. The abundance of the 1.2 kb endogene RNA suggests that this may be the result of the most common initial cleavage site. A putative poly(A) signal (5′-AATTGAA-3′) is present 33–27 nucleotides upstream of this 3′ UTR cleavage site, which may account for why some RNAs cleaved at this site are polyadenylated. This explanation implies that the cleavage occurs in the nucleus, where polyadenylation also occurs. We note that this putative preferred RNA cleavage site follows a G residue, which is also the case for other RNA endonucleolytic cleavage sites (Table 1B) (Binder et al., 1994; Goodwin et al., 1996; Scheper et al., 1996). The boundaries of the short endogene RNA fragments surviving preferentially in white-flowered plants showing severe cosuppression

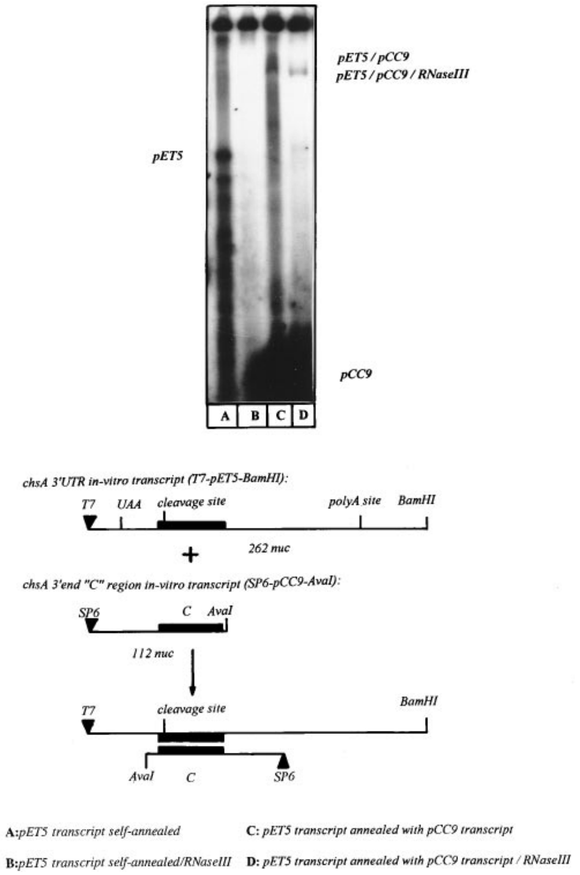

Figure 6. In Vitro Transcription, Annealing, and Endonucleolytic Cleavage of Complementary *chsA* RNA Regions

^{32}P-labeled in vitro transcripts were either self-annealed or cross-annealed and were separated on a 5% nondenaturing PAA gel. (A) A ^{32}P-labeled sense transcript of the complete *chsA* 3′ UTR was self-annealed with a 10-fold excess of its unlabeled complementary transcript. (B) An equivalent aliquot of this self-annealed RNA was incubated with dsRNA- specific RNaseIII. (C) A ^{32}P-labeled sense transcript of the complementary region located at the 3′ end of the *chsA* coding region was annealed with a 10-fold excess of unlabeled sense transcript of the complete *chsA* 3′ UTR. (D) An equivalent aliquot of the RNA mix used in (C) was treated with RNaseIII.

imply that a second cleavage occurs upstream within the *chsA* coding region (Figure 3). The preferential survival of the RNA products of these two endonucleolytic cleavages is especially noteworthy. The RNAs presumably adopt secondary structures that are more resistant to RNases relative to other segments of the *chsA* RNAs. We have shown that some RNA structures formed in vitro between complementary sequences in this RNA segment can resist RNase III degradation unlike other RNA duplexes (Figure 6). The same RNA cleavages occur and the same RNA fragments survive degradation in white flower tissue of plants similar to the nontransgenic variety Red Star (Mol et al., 1983). This finding strongly supports the hypothesis that the transgene *chsA* RNA present in transgenic lines acts only as a trigger for the induction of an existing *chsA* RNA-specific, posttranscriptional control mechanism.

A Model for Cosuppression Involving Cycles of RNA Pairing and Endonucleolytic Cleavage

If *chsA* RNAs are susceptible to a series of cleavages, how can the presence of transgenes stimulate these cleavage processes? Jorgensen et al. (1996) have shown that cosuppression increases with more copies of the gene. Here we show that reversion from white to stable purple flowers in the epigenetic formation of C002 from C001 is associated with a large reduction in the levels of transgene RNA in leaves. It is unlikely that high endogene expression is required to maintain the state of cosuppression in transgenic plants because cosuppression of transgene RNAs is observed in tissues during plant development when endogene expression is low. Endogene expression occurs only in the L1 epidermal cells, but transgene RNA levels show suppression also in flower petal L2 layers. We therefore conclude that transgene RNA is sufficient to maintain the state of cosuppression, even though cosuppression might be enhanced by the presence of endogene RNA, for example in epidermal cells of purple-white patterned flowers. However, we concluded earlier that high levels of *chsA* alone are insufficient to promote cosuppression. We therefore suggest that aberrant poly(A)$^-$ *chsA* RNA is the active inducer of cosuppression.

Much long poly(A)$^-$ *chsA* RNA accumulates in plants possessing active transgenes and in plants similar to the variety Red Star. This conclusion is based on the relatively low levels of full-length poly(A)$^+$ RNA relative to 5′ and 3′sections of RNA in white versus purple tissues (Figure 2). We do not know what induces the production of poly(A)$^-$ RNA fragments but suspect that it may be the localized accumulation of high levels of RNA. The presumed preferential sites of endonucleolytic cleavage of endogene RNA lie within 43-base paired segments of the coding regions and 3′ UTR sequences that are 80% complementary. These cleavages in endogene RNA might therefore result from the recognition of structures formed by intermolecular pairing between the coding sequence on aberrant fragments of RNA and the complementary 3′ UTR sequence of the mRNA. Cleavage of this paired RNA, as shown in Figure 7, would produce the 1.2 kb form of endogene mRNA observed in Figure 2 and a shorter poly(A)$^-$ aberrant RNA. The 1.2 kb endogene RNA has a poly(A) addition sequence and could explain why some of these molecules are repolyadenylated. On the assumption that the 1.2 kb endogene RNAs are formed in this way, we predict that the pairing and cleavages take place in the nucleus; otherwise, repolyadenylation could not take place. Poly(A)$^-$ endogene products from this pairing–cleavage reaction presumably would not be actively transported out of the nucleus because of lack of a poly(A) tail and therefore could base pair with the 3′ UTR complementary sequences of other full-length endogene mRNAs to produce, following endonucleolytic cleavages, more of the 1.2 kb endogene RNAs and the 304-base fragments observed (Figure 7). We therefore propose that loss of *chsA* RNA in floral cosuppression occurs by means of pairing–cleavage cycles between poly(A)$^-$ endogene or transgene RNA molecules that fail to progress out of the nucleus efficiently and nuclear full-length mRNA

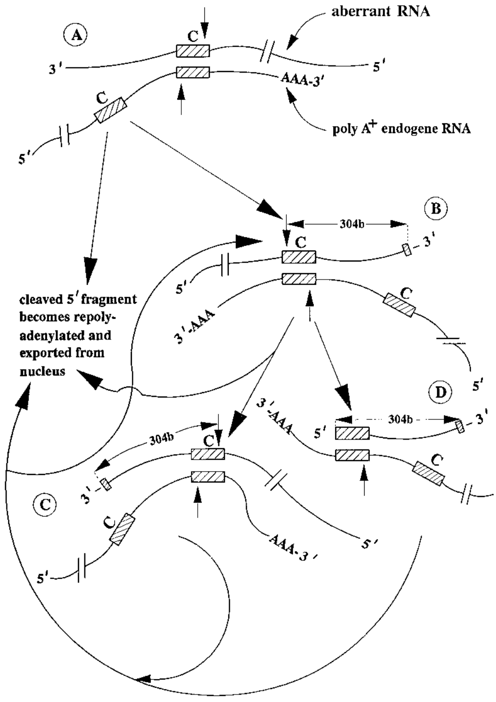

Figure 7. A Cyclic Model of RNA Degradation Based on Complementary RNA Pairing and Endonucleolytic Cleavage

The process is initiated by the local accumulation of aberrant *chsA* RNAs, which can be any *chsA* RNA, from endogene or transgene, whose "normal" export from the nucleus and translation are inefficient or prevented because of structural aberrations. The aberrant RNA base pairs with the complementary sequence in the 3′ UTR of an endogene RNA (A). Endonucleolytic cleavages occur at specific sites (short line pairs) to generate two truncated molecules. The truncated endogene RNA can be repolyadenylated and exported from the nucleus to form the observed shorter poly(A)$^+$ endogene RNA. Alternatively, it can pair with the 3′ UTR sequence of another *chsA* endogene RNA (B). Specific endonucleolytic cleavages of this duplex lead to the observed 304-base RNA and a long *chsA* RNA lacking its 3′ end. This latter RNA can be repolyadenylated and exported from the nucleus, or it can pair with the 3′ UTR sequence of another *chsA* endogene RNA (C), as in (B). The 304 bp product from (B) can also pair with another endogene RNA (D) to produce another long RNA lacking its 3′ end. Thus the products of one pairing–cleavage event are potential substrates for two others. The same cycle can also take place between RNAs in the cytoplasm.

products, as a result of the sequence complementarity between the coding and 3′ UTR sectors. We have shown (Figure 6) that RNA–RNA pairing in vitro between these sectors can lead to structures that are cleaved by E. coli dsRNA-specific RNase III but are not degraded extensively like RNA–RNA duplexes between completely complementary RNA sequences. However, it remains unknown whether RNase III–like enzymes act in vivo as an endonucleolytic component of the observed *chsA* RNA-specific RNA degradation system.

Once the process of *chsA* RNA–specific degradation is initiated, it could eliminate all of the endogene full-length *chsA* RNA rapidly because the products of each reaction are substrates for another round of reactions, as shown in Figure 7. The proposed "autoregulatory" degradative cycle is thus attractive to explain (1) how the observed relatively large proportions of poly(A)$^-$ *chsA* RNA are generated; (2) how phenotypic switches from purple to white tissue occur rapidly; and (3), if the short RNA molecules survive through the cell cycle, how the state of cosuppression is somatically inherited. The attractions of an autoregulatory system to explain gene silencing observations have been described by Meins and Kunz (1994). In addition, the 1.4 kb endogene RNAs with two sites capable of undergoing complementary pairing with transgene RNA or with poly(A)$^-$ cleavage products would be expected to undergo degradation more rapidly than 1.2 kb endogene and transgene 1.4 kb mRNAs, which have only one site, as is frequently observed (Figure 2 and unpublished data). Although we suggest that pairing–cleavage cycles occur in the nucleus, it is also likely that they occur in the cytoplasm, if the conformation of the RNAs in the mRNPs allows intermolecular interactions and the relevant RNases are present.

The origins of cosuppression in this model are the observed aberrant *chsA* poly(A)$^-$ RNA molecules. They occur in nontransgenic situations, but their concentration is enhanced in transgenic lines or in conditions of high levels of *chsA* endogene RNA. In this regard it is noteworthy that low levels of the 1.2 kb poly(A)$^+$ endogene RNA molecules are seen in wild-type Petunia and in plants similar to the variety Red Star.

The proposed RNA degradation scheme is based on the existence of complementary sequences in *chsA* mRNA that are located at the mRNA 3′ end. Other examples exist where interactions between the 3′ UTR and other mRNA sequences are involved in the regulation of RNA cleavage by guiding RNA cleavage (Wightman et al., 1993). However, similar complementary sequences that promote RNA–RNA pairing may exist in other regions of a mRNA. Such complementarity may have been selected as a component of an RNA turnover control system by intra- or intermolecular RNA pairing.

Why do some transgenic plants with active *chsA* transgenes have stable purple flowers? The reason could be that the transgenes are localized in nuclear sectors that give rise to less poly(A)$^-$ *chsA* RNA, that transcription rates are insufficiently high to accumulate enough *chs* RNA in the nucleus, or that the mRNAs of endogenes and transgenes are in different regions of the nucleus. Epigenetic switches in cosuppression may therefore be due to changes in nuclear organization or transgene expression, as noted for C001 and C002 here. They occur most frequently in meristems and affect L1 and L2 layers simultaneously, possibly because meristems are where resetting of nuclear organization and transgene or endogene chromatin occurs preferentially. The state of cosuppression may also be activated by conditions that activate *chsA* endogenes. A boost to the level of endogene RNA would enhance the pool of molecules able to interact and drive the cycle to a new steady state of RNA degradation. It is therefore relevant that cosuppression can be influenced by external conditions also known to influence *chsA* expression (Jorgensen and Napoli, 1996).

The differences in floral patterns observed for different lines displaying *chsA* cosuppression may reflect the differential expression of transgenes in response to special gradients of transgene transcription factors in sectors of the meristem (Jorgensen, 1995; Jorgensen et al., 1996). However, from the model proposed here they may also reflect the patterns of endogene expression, the locations of transgene and endogene *chsA* RNAs in the nucleus, the pattern of accumulation of poly(A)$^-$ *chsA* RNAs, or conceivably the patterns of movement of small cleavage products of *chsA* RNAs between cells in the meristem.

Jorgensen et al. (1996) have concluded from a large study of transgenic plants that single copies of transgenes stimulate cosuppresion only during flower development (i.e., when endogene RNA is activated), whereas multiple copies of transgenes, and especially inverted repeat copies, enhance the probability of more extensive cosuppression and, in particular, cosuppression in leaves and stems. These structures might promote aberrant transgene RNAs. Our model implies that transgene expression is essential for transgenes to stimulate the occurrence of cosuppression. However, Van Blokland et al. (1994) have reported that promoterless transgenes can stimulate cosuppression. We cannot explain this observation, but it may be due to transcription from another promoter at some point in development to initiate the RNA pairing–cleavage cycle or due to generation of an abnormal RNA in low quantities that has a very high potential of being poly(A)$^-$ and thereby initiating the endogene RNA pairing–cleavage cycle. If, as we predict here, RNA–RNA pairing exists in the nucleus to drive the phenomenon of cosuppression, RNA–DNA pairing might also occur to cause epigenetic changes to the genes. Elsewhere we will present data on such epigenetic changes that correlate with cosuppression.

Finally, our data and the model described here are also consistent with recent reports about cases of posttranscriptional gene silencing in Neurospora crassa (Cogoni et al., 1996) and in virus-resistant transgenic plants (Baulcombe and English, 1996; English et al., 1996; Goodwin et al., 1996). Dougherty et al. (1994) and Smith et al. (1994) have offered an explanation for the means by which cytoplasmic viral RNA replication is inhibited in transgenic plants possessing low levels of transgene mRNA homologous to the viral RNA. Our model, derived from the data on chalcone synthase, has many similarities to theirs; however, having defined an RNA degradation product carrying a complementary sequence, we favor the conclusion that cytoplasmic RNA pairing–cleavage cycles are also the basis of transgene-promoted virus resistance. The regions of complementarity within RNA molecules would be expected to differ from case to case and may not be restricted to 3′ end positions. There has been considerable debate on whether antisense RNA is involved in posttranscriptional sense-gene silencing (Grierson et al., 1991; Mol et al., 1991; Flavell, 1994). In the model proposed here, complementary RNA is involved, but it is inherent in the sense transcript.

Experimental Procedures

Transgenic Plants

The transgenic Petunia hybrida plants used in our experiments were kindly provided by Dr. John Bedbrook (DNA Plant Technology Corporation, Oakland, California) and Dr. Richard Jorgensen (Department of Environmental Horticulture, University of California, Davis). The original transformants described by Napoli et al. (1990) and Jorgensen et al. (1996) were backcrossed by us with wild-type plants V26 to give C001, C002 (from CHS38), C423 (from CHS244), and C356 (from CHS223). A distinct description of the transgenic Petunia lines including the transgene copy numbers can be found in Jorgensen et al. (1996). In our comparative analyses we used the nontransgenic Petunia F1 Razzle Dazzle (Suttons Seeds Ltd., UK) with a flower pattern similar to that of the variety Red Star (Mol et al., 1983). Plants of this variety show white sectors in purple flower tissue like that of purple-white patterned transgenic plants.

chsA Transgene Construction and Plant Transformations

The *chsA* transgene construction and plant transformations were carried out at DNA Plant Technology Corporation and at the Department of Environmental Horticulture, University of California, Davis, as described in Napoli et al. (1990) and Jorgensen et al. (1996).

Northern and Dot-Blot RNA Analyses

Northern and dot-blot RNA analyses were carried out by following the Stratagene instruction manual. Total RNA was isolated as described by Napoli et al. (1990) from freshly harvested leaves and flowers immediately frozen in liquid nitrogen. The age of the plants used in our analyses varied between 6 weeks to 3 months. For Northern analyses, 10 μg of total RNA was separated on 1% agarose–20% formaldehyde gels. All hybridization probes were labeled by random priming using [α-^{32}P]deoxycytosine triphosphate ([α-^{32}P]dCTP) (Amersham).

RT-PCR

RT-PCR analyses were performed following the RACE protocol (Frohman et al., 1988) with some modifications. One microgram of total RNA dissolved in sterile water was mixed with 2 μl of 10× PCR buffer (100 mM Tris-HCl [pH 8.3], 500 mM KCl, 25 mM $MgCl_2$, 0.5% Nonidet P-40), 2 μl of 5 mM deoxynucleotide triphosphate mix (prepared by mixing equal volumes of 20 mM deoxynucleotides, Boehringer Mannheim), 2 μl of 50 μM RACE oligo dT-adaptor (B26-B25) or 2 μl of 20 μM primer complementary to sense RNA, and water to a final volume of 19 μl. The mixture was heated at 65°C for 5 min and rapidly cooled on ice. After the addition of 1 μl of RT (Moloney murine leukemia virus [M-MLV] RT, GIBCO BRL), the cDNA synthesis was carried out at 52°C for 30 min. The RT was subsequently inhibited by heating the samples at 99°C for 1 min. Aliquots of the resulting cDNA were used for PCR with final primer concentrations of 0.5 μM and 0.5 μl Taq-polymerase (Boehringer Mannheim). The PCR reactions were carried out for 18 or 35 cycles, respectively (30 s at 94°C, 30 s at 60°C, 1 min at 72°C) and a final extension at 72°C for 10 min. Ten microliters of the total reaction volumes were used for electrophoresis on 1.5%–2.5% agarose gels in Tris-borate-EDTA buffer. The DNA was transferred with 20× saline–sodium citrate onto nylon membrane and hybridized with ^{32}P-labeled probes.

Linear PCR

For linear PCR reactions, cDNA aliquots were amplified in a total reaction volume of 20 μl using 50 nM of a single ^{33}P–end-labeled oligonucleotide for 18 PCR cycles (20 s at 94°C, 30 s at 60°C, 30 s at 72°C) and a final extension at 72°C for 10 min. Two microliters of each reaction was separated on 6% PAA-urea sequencing gels.

PCR Sequencing of DNA Fragments

Dideoxy-PCR sequencing of DNA fragments isolated from agarose gels was carried out according to the protocol of Murray (1989). Fifty nanograms of DNA template and 50 nM of a ^{33}P–end-labeled primer were used for 18 cycles of amplification (performed as for linear PCR) without a final extension at 72°C. Two microliters of of the resulting sequencing reaction were separated on 6% PAA-urea sequencing gels.

In Vitro Transcription, Transcript Annealing, and RNase III Cleavage

PCR fragments for the region of complementarity within the *chsA* 3′ end coding region and for the complete *chsA* 3′ UTR were separately ligated with SmaI-cut and T-tailed pSPT18 vector DNA (Boehringer Mannheim) from which the recombinant plasmids pCC9 and pET5 resulted. The in vitro transcription reactions were carried out according to the instructions of the supplier by using either T7 or SP6 RNA polymerase and 50 μCi [α-^{32}P]CTP (Amersham) or unlabeled CTP. After phenol extraction and ethanol precipitation, the resulting in vitro transcripts were mixed in a ratio of 1 to 10 (labeled to unlabeled). The mixed transcripts were heated at 90°C for 10 min followed by an incubation at 30°C for 1 hr. Aliquots of the annealing reactions were incubated with 1 Kunitz unit of E. coli RNase III at 30°C for 20 min in a buffer containing 60 mM KCl, 10 mM MgCl$_2$, and 5 mM Tris-HCl (pH 7.5). Products of the in vitro reactions were then separated on 5% nondenaturing PAA gels.

Acknowledgments

We thank Dr. John Bedbrook (DNA Plant Technology Corporation, Oakland, California) and Dr. Richard Jorgensen (University of California, Davis) for the transgenic Petunia plants and for encouraging discussions when we started the research on *chsA* cosuppression. We are grateful to Dr. Allen Nicholson (Wayne State University) for the gift of E. coli RNase III and for helpful advice. We also thank Professor William Thompson (Raleigh, North Carolina) for stimulating discussions and support during his visit to the John Innes Centre in Norwich. We are grateful to Dr. Peter Shaw and Dr. Tristan Dyer of the John Innes Centre for critical reading of the manuscript. Our research was financed by the Biotechnology and Biological Sciences Research Council, United Kingdom.

Received August 27, 1996; revised January 31, 1997.

References

Baulcombe, D.C., and English, J.J. (1996). Ectopic pairing of homologous DNA and post-transcriptional gene silencing in transgenic plants. Curr. Opin. Biotech. *7*, 173–180.

Binder, R., Horowitz, J.A., Basilion, J.P., Koeller, D.M., Klausner, R. D., and Harford, J.B. (1994). Evidence that the pathway of transferrin receptor messenger-RNA degradation involves an endonucleolytic cleavage within the 3′ UTR and does not involve poly(A) tail shortening. EMBO J. *13*, 1969–1980.

Cogoni, C., Irelan, J.T., Schumacher, M., Schmidhauser, T.J., Selker, E.U., and Macino, G. (1996). Transgene silencing of the al-1 gene in vegetative cells of Neurospora is mediated by a cytoplasmic effector and does not depend on DNA-DNA interactions or DNA methylation. EMBO J. *15*, 3153–3163.

De Carvalho Niebel, F., Frendo, P., Van Montagu, M., and Cornelissen, M. (1995). Post-transcriptional cosuppression of beta-1,3-glucanase genes does not affect accumulation of transgene nuclear mRNA. Plant Cell *7*, 347–358.

Depicker, A., Ingelbecht, I., van Houdt, H., de Loose, M., and van Montagu, M. (1996). Post-transcriptional reporter transgene silencing in transgenic tobacco. In Mechanisms and Applications of Gene Silencing, D. Grierson, G.W. Lycett, and G.A. Tucker, eds. (Nottingham, UK: Nottingham University Press), pp. 71–84.

Dougherty, W.G., Lindbo, J.A., Smith H. A., Parks, T.D., Swanley, S., and Proebstung, W.M. (1994). RNA-mediated virus resistance in transgenic plants: exploration of a cellular pathway possibly involved in RNA degradation. Mol. Plant-Microbe Interact. *7*, 544–552.

English, J.J., Mueller, E., and Baulcombe, D.C. (1996). Suppression of virus accumulation in transgenic plants exhibiting silencing of nuclear genes. Plant Cell *8*, 179–188.

Flavell, R.B. (1994). Inactivation of gene expression in plants as a consequence of specific sequence duplications. Proc. Natl. Acad. Sci. USA *91*, 3490–3496.

Frohman, M.A., Dush, M.K., and Martin, G.R. (1988). Rapid production of full-length cDNAs from rare transcripts: amplification using a single gene-specific oligonucleotide primer. Proc. Natl. Acad. Sci. USA *85*, 3998–4002.

Goodwin, J., Chapman, K., Swanley, S., Parks, T.D., Wernsman, E.A., and Dougherty, W.G. (1996). Genetic and biochemical dissection of transgenic RNA-mediated virus resistance. Plant Cell *8*, 95–105.

Grierson, D., Fray, R.G., Hamilton, A.J., Smith, C.J.S., and Watson, C.F. (1991). Does co-suppression of sense genes in transgenic plants involve antisense RNA? Trends Biotechnol. *9*, 122–123.

Hamilton, A.J., Brown, S., and Grierson, D. (1996). Post transcriptional gene silencing in tomato. In Mechanisms and Applications of Gene Silencing, D. Grierson, G.W. Lycett, and G.A. Tucker, eds. (Nottingham, UK: Nottingham University Press), pp. 105–117.

Jorgensen, R.A. (1995). Cosuppression, flower color patterns, and metastable gene expression states. Science *268*, 686–690.

Jorgensen, R.A., and Napoli, C.A. (1996). A responsive regulatory system is revealed by sense suppression of pigment genes in Petunia flower. In Genomes of Plants and Animals: Proceedings of the 22nd Stadler Genetics Symposium, J.P. Gustafson and R.B. Flavell, eds. (New York: Plenium Press), pp. 159–176.

Jorgensen, R.A., Cluster, P.D., English, J., Que, Q., and Napoli, C. (1996). Chalcone synthase cosuppression phenotypes in petunia flowers: comparison of sense vs. antisense constructs and single copy vs. complex T-DNA sequences. Plant Mol. Biol. *31*, 957–973.

Li, H.-L., Chelladurai, B.S., Zhang, K., and Nicholson, A.W. (1993). Ribonuclease III cleavage of a bacteriophage T7 processing signal: divalent cation specificity, and specific anion effects. Nucl. Acids Res. *21*, 1919–1925.

Martin, C.R. (1993). Structure, function, and regulation of the chalcone synthase. Int. Rev. Cytol. *147*, 233–284.

Matzke, M.A., and Matzke, A.J. M. (1995). How and why do plants inactivate homologous (trans)genes? Plant Physiol. *107*, 679–685.

Meins, F. Jr., and Kunz, C. (1994). Silencing of chitinase expression in transgenic plants: an autoregulatory model. In Homologous Recombination and Gene Silencing in Plants, J. Paszkowski, ed. (Netherlands: Kluwer Academic Publishers), pp. 335–348.

Meyer, P., ed. (1995). Gene Silencing in Higher Plants and Related Phenomena in Other Eukaryotes (Berlin-Heidelberg: Springer-Verlag).

Meyer, P., and Heidmann, I. (1994). Epigenetic variants of a transgenic petunia line show hypermethylation in transgene DNA: an indication for specific recognition of foreign DNA in transgenic plants. Mol. Gen. Genet. *243*, 390–399.

Mol, J., van Blokland, R., and Kooter, J. (1991). More about co-suppression. Trends Biotechnol. *9*, 182–183.

Mol, J.N.M., Schram, A.W., de Vlaming, P., Gerats, A.G.M., Kreuzaler, F., Hahlbrock, K., Reif, H.J., Veltkamp, E. (1983). Regulation of flavonoid gene expression in Petunia hybrida: description and partial characterisation of a conditional mutant in chalcone synthase gene expression. Mol. Gen. Genet. *192*, 424–429.

Murray, V. (1989). Improved double-stranded DNA sequencing using linear polymerase chain reaction. Nucl. Acids Res. *17*, 8889.

Napoli, C., Lemieux, C., and Jorgensen, R. (1990). Introduction of a chimeric chalcone synthase gene into petunia results in reversible co-suppression of homologous genes in trans. Plant Cell *2*, 279–289.

Scheper, W., Holthuizen, P.E., and Sussenbach, J.S. (1996). The cis-acting elements involved in endonucleolytic cleavage of the 3′-UTR of human IGF-II messenger-RNAs bind a 50 kDa protein. Nucl. Acids Res. *24*, 1000–1007.

Smith, H.A., Swaney, S.L., Parks, T.D., Wernsman, E.A., and Dougherty, W.G. (1994). Transgenic plant virus resistance mediated by untransalatble sense RNAs: expression, regulation and fate of nonessential RNAs. Plant Cell *6*, 1441–1453.

Van Blokland, R., Van der Geest, N., Mol, J.N.M., and Kooter, J.M. (1994). Transgene-mediated suppression of chalcone synthase expression in Petunia hybrida results from an increase in RNA turnover. Plant J. *6*, 861–877.

Van der Krol, A.R., Mur, L.A., Beld, M., Mol, J.N.M., and Stuitje, A.R. (1990). Flavonoid genes in petunia: Addition of a limited number of gene copies may lead to a suppression of gene expression. Plant Cell *2*, 291–299.

Wightman, B., Ha, I., and Ruvkun, G. (1993). Posttranscriptional regulation of the heterochronic gene *lin-14* by *lin-4* mediates temporal pattern formation in C. elegans. Cell *75*, 855–862.

Zuker, M., and Stiegler, P. (1981). Optimal computer folding of large RNA sequences using thermodynamics and auxiliary. Nucl. Acids Res. *9*, 133–148.